NOVEM 2018
Noise and vibration emerging methods
The 6th conference, 7 – 9 May 2018
Ibiza – Spain

CONSTRUCTION AND CHARACTERIZATION OF AN OMNIDIRECTIONAL PARAMETRIC LOUDSPEAKER CONSISTING OF ULTRASOUND TRANSDUCERS SET ON A SPHERE

Marc Arnela[1*], Patricia Sánchez-Martín[1], Marcos Hervás[1], Joan Camps[1], Oriol Guasch[1], Carme Martínez-Suquía[1] and Rosa Ma Alsina-Pagès[1]

[1]GTM Grup de recerca en Tecnologies Mèdia, La Salle, Universitat Ramon Llull
C/ Quatre Camins 30, Barcelona 08022, Catalonia
[*]Email: marnela@salleurl.edu

ABSTRACT

Standard omnidirectional sound sources typically consist of conventional loudspeakers arranged in a dodecahedral configuration. For such devices, a microphone in a circular trajectory around the source should measure a constant sound pressure level. However, the directivity of loudspeakers sharpens with increasing frequency. The omnidirectionality of the source therefore wanes at the high range of the spectrum, the effect being very noticeable at the vertices of the dodecahedron.

In this work it is proposed to circumvent this problem by exploiting the parametric acoustic array (PAA) phenomenon. An omnidirectional parametric loudspeaker (OPL) is built by setting hundreds of small piezo-electric transducers (PZTs) on a sphere. Each PZT emits a collimated primary beam consisting of a carrier ultrasonic wave modulated by an audible signal. Thanks to non-linear propagation of sound in air, the air itself demodulates the primary beam giving rise to an emission cone of audible acoustic pressure (secondary field). For an appropriate distribution of PZTs on the sphere, the emission cones are such that an omnidirectional acoustic pressure field is recovered. In practice, a balance is required between an optimal PZT distribution and the practical needs for a prototype construction. Our choice has been to follow an equal-area partitioning strategy on the sphere surface, which aligns the PZTs in parallels and performs almost as well as an optimal PZT distribution, as shown by theoretical prediction models. The parallel PZT alignment strongly facilitates the PZT welding process and setting the cable circuitry. An equal-area distributed OPL prototype has been built resorting to 3D printing for the spherical casing. The prototype has been tested in an anechoic chamber showing a remarkable omnidirectional character for all frequencies.

1 INTRODUCTION

Omnidirectional sound sources are needed in many acoustic tests, such as the measurement of the reverberation time of a room, the sound insulation of a partition, or the absorption coefficient of a material sample in a reverberation chamber. These sound sources are typically built by arranging 12 conventional loudspeakers in a dodecahedron (see Figure 1a), so that sound waves can be emitted in all directions. Ideally, one should measure a constant sound pressure level (SPL) when completing a circular trajectory around the dodecahedron. However, loudspeakers become more directive with frequency. This results in dips of the SPL when crossing the vertices of the dodecahedron and omnidirectionality gets lost at the mid-high frequency range.

An alternative to solve that problem which resorted to the Parametric Acoustic Array (PAA) phenomenon (see e.g., [1–3]) was first proposed in [4]. In that work, a so-called Omnidirectional Parametric Loudspeaker (OPL) was built, which consisted of hundreds of small piezo-electric transducers (PZTs) set on a sphere. Each of those transducers emit an ultrasonic carrier wave modulated with an audible signal. The air itself demodulates the total emitted signal thanks to non-linear propagation effects, resulting in a strongly focused beam of audible sound in front of the transducer. Given that the dimensions of the PZTs are much smaller than those of regular loudspeakers, hundreds of PZTs can be set on the surface of the sphere (see Figure 1b). For a proper OPL design, if one follows a circular trajectory around the OPL with a microphone, the transition from one PZT beam to another will be very smooth and no SPL differences should be perceived. This shall solve the problem encountered at the vertices of conventional dodecahedron loudspeakers, the price to be paid being less intense sound at low frequencies.

In this work we present the design and construction of a new prototype of OPL that improves by far the performance of the preliminary model in [4], see Figure 1b. The paper is organized as follows: in section 2 we overview the theory behind the PAA phenomenon. Section 3 is devoted to the design and construction of the OPL. It reports which criteria was used to select the PZT model and how those were distributed on the spherical surface. Details are also given on how the spherical casing was built, as well as on the OPL circuitry. Directivity measurements for the OPL are provided in section 4. Finally, the conclusions are drawn in section 5.

(a) Conventional dodecahedral source of sound

(b) Proposed omnidirectional parametric loudspeaker (OPL)

Figure 1. Omnidirectional sound sources

2 PARAMETRIC ACOUSTIC ARRAY THEORY

Let us briefly review the foundations of the PAA phenomenon, first derived in Westervelt's original paper [1]. Westervelt considered sound propagation in a thermoviscous fluid described by the equation

$$\frac{1}{c_0^2}\frac{\partial^2 p}{\partial t^2} - \nabla^2 p = \frac{\delta}{c_0^4}\frac{\partial^3 p}{\partial t^3} + \frac{\beta}{\rho_0 c_0^4}\frac{\partial^2 p^2}{\partial t^2}, \tag{1}$$

where p represents the acoustic pressure, c_0 and ρ_0 respectively stand for the speed of sound and the ambient density, and δ and β designate the sound diffusivity and the non-linearity parameter. The left hand side (l.h.s) of (1) can be recognized as the standard lossless linear wave equation, whereas the first term in the right hand side (r.h.s) accounts for thermoviscosity and the second one for non-linear propagation effects.

For weak non-linearity, one may attempt a quasilinear approximation to (1) (see e.g., [2]) by decomposing the acoustic pressure as $p = p_1 + p_2$ ($|p_2| \ll |p_1|$), with the primary field p_1 satisfying the linearized version of (1), and the secondary one, p_2, arising as a non-linear byproduct of p_1. Substituting $p = p_1 + p_2$ into (1) results in the following linear equations for the primary and secondary fields,

$$\frac{1}{c_0^2}\frac{\partial^2 p_1}{\partial t^2} - \nabla^2 p_1 - \frac{\delta}{c_0^4}\frac{\partial^3 p_1}{\partial t^3} = 0, \tag{2a}$$

$$\frac{1}{c_0^2}\frac{\partial^2 p_2}{\partial t^2} - \nabla^2 p_2 - \frac{\delta}{c_0^4}\frac{\partial^3 p_2}{\partial t^3} = \frac{\beta}{\rho_0 c_0^4}\frac{\partial^2 p_1^2}{\partial t^2}. \tag{2b}$$

It can be easily checked that the solution to (2a) consists of attenuated traveling waves which, once squared, act as a source term for equation (2b) governing the secondary pressure field p_2. If the primary field is made of two collimated plane waves emitted by a PZT in the positive z-axis,

$$p_1 = P_1 e^{-\alpha_1 z}\cos(w_1 t - k_1 z) + P_2 e^{-\alpha_2 z}\cos(w_2 t - k_2 z), \tag{3}$$

($\alpha_i = \delta\omega_i^2/2c_0^3$, $i = 1, 2$, being the wave attenuation factors), the squared amount p_1^2 in the source of (2b) will give place to a term involving twice the frequencies $2\omega_1$ and $2\omega_2$, another one containing the frequency summation $\omega_1 + \omega_2$, and a last one with the difference frequency $\omega_d = |\omega_1 - \omega_2|$. Choose ω_1 and ω_2 close together and to lie in the ultrasonic range, say, for instance, 40 kHz and 41 kHz, and the difference frequency component (secondary field p_2) would result in a 1 kHz audible sound. This is the essential behind the PAA, where in typical applications the primary field consists of a plane wave made from an ultrasonic carrier modulated by a broadband signal in the audible range (see e.g., [5, 6]).

Inserting (3) into (2b) solely retaining the difference frequency component in the source term and solving the equation using the standard Green function approach, yields the celebrated Westervelt expression for the audible secondary pressure, p_d, at a far-field point (r_0, θ_0) (see [e.g., 1, 2, 7]),

$$p_d(r_0, \theta_0) = K S_0 P_1 P_2 D_W(\theta_0)\cos(w_d t - k_d r_0 - \phi), \tag{4}$$

with

$$K = \frac{\beta\omega_d^2}{4\pi\rho_0 c_0^4 r_0(\alpha_1 + \alpha_2)}, \quad D_W(\theta_0) = \frac{\alpha_1 + \alpha_2}{\sqrt{(\alpha_1 + \alpha_2)^2 + k_d^2(1 - \cos\theta_0)^2}}, \quad \tan\phi = \frac{k_d(1 - \cos\theta_0)}{\alpha_1 + \alpha_2}. \tag{5}$$

In (5) r_0 is the distance from the PZT to the observer, θ_0 is the sustained angle between the PZT emission axis and the position of the observer, and k_d is the wave number of the difference frequency wave, $k_d = \omega_d/c_0$. $D_W(\theta)$ is known as the Westervelt directivity and is responsible for a very sharp secondary audible field without lobes, which is at the core of the audio spotlight applications [6].

When applied to determine the far field pressure of parametric loudspeaker arrays (PLAs), however, equation (4) suffers from severe limitations, the assumption of collimated primary waves being too stringent. Several proposals can be found in literature to remedy that situation, starting with the incorporation of the product of the primary field directivities into (4) (see [7] and also [3, 8] for a review on further approaches). Just a few years ago, an alternative model was proposed to deal with PLAs consisting of arrays of PZTs with beam widths up to 80° [9]. The model provides the following prediction formula for the far field, to be compared to (4),

$$p_d(r_0, \theta_0) = K \cos\left(w_d t - k_d r_0\right) \int_{-\psi_0}^{\psi_0} D_1(\psi) D_2(\psi) D_W(\theta_0 - \psi)\, d\psi, \tag{6}$$

ψ_0 being half the PZT beam width. As seen from (6), in this case the directivity of the audible field is obtained from the convolution between Westervelt's directivity and the product of the primary field directivities. The convolution model was reported to provide better predictions than previous models for planar PLAs in [9]. Very recently, the convolution model has been generalized to deal with PLAs set on curved surfaces [10], which could be useful to predict the performance of several non-conventional PLA devices ([11–13]). In particular, the generalized convolution model in [10] has been used as a guidance for the design of the OPL prototype reported in this paper.

3 CONSTRUCTION OF AN OMNIDIRECTIONAL PARAMETRIC LOUDSPEAKER

3.1 Design

Several parameters need to be considered when designing an omnidirectional parametric loudspeaker made of hundreds of PZT transducers on a sphere. Probably the most important ones are the transducer model, the sphere radius, and the transducer distribution on the sphere surface. Af-

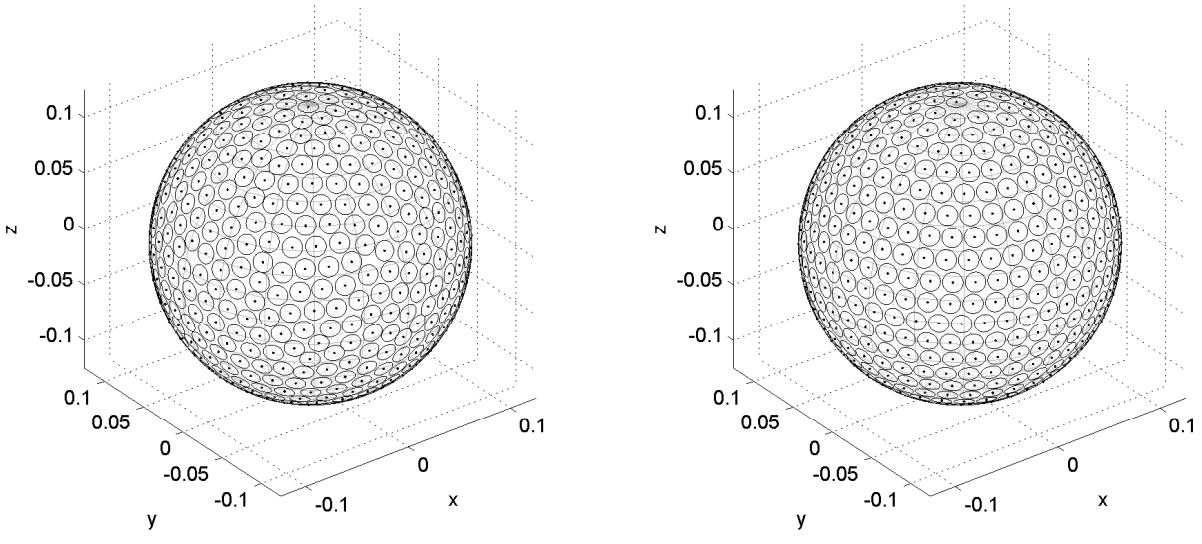

Figure 2: Distribution of PZTs on the OPL (a) force-equilibrium distribution (b) equal-area partitioning

ter experimentally testing many commercial PZT transducers on the market, we have selected the Multicomp 16mm Transmitter (ST160), since it presented high pressure levels with a quite wide directivity pattern at a reasonable price. Knowing that the circular base of this transducer has a radius of $r = 0.008$ m, the next problem to address is how to distribute all transducers on the spherical surface.

Looking for an optimal distribution of points on the surface of a sphere is a classical, non simple problem [14]. Some approaches to it rely on minimizing an associated energy problem [14, 15], or on supposing that all points are connected by struts and finding a force equilibrium solution [16]. The last procedure, hereinafter called the *force-equilibrium* PZT distribution, has been first adopted in this work. In Figure 2a we show a realization of such a distribution in a sphere of radius $R = 0.125$ m. Every circle on the surface represents a PZT. They have all been set a distance of 0.0001 m apart to avoid contact. This configuration gave a total of 755 PZTs.

To achieve an optimal, or at least very efficient, distribution of PZTs is desirable, but simplicity of construction is also essential. For this reason, another method to set the PZTs on the sphere has been investigated. The alternative configuration consists in dividing each parallel band of the sphere into N_{PZT} equal-areas. The parallel bands have the width of a PZT, and each band is filled with PZTs, again with an inter-separation of 0.0001 m. Figure 2b shows this distribution, which will be hereafter refereed to as the *equal-area* partition, on the same sphere used for the *force-equilibrium* case. 750 PZTs fill the sphere for the equal-area partitioning scheme, as compared to the 755 of the *force-equilibrium* distribution. The advantage of the equal-areas distribution is, however, that its strongly facilitates the cable circuitry and the welding process. The price to pay: a worse transducer distribution which may affect the directivity pattern.

Some theoretical predictions were performed to analyze the performance of the force-equilibrium and equal-area partition strategies [10]. In Figure 3 we show some of the results corresponding to the far-field SPL obtained for a difference frequency of 2 kHz, at 4 m from the OPL surface for three different half orbits (from top to bottom: an orbit around the equator, around a meridian, and with an inclination of 45°; the three trajectories crossing at 90^o). As can be observed, the secondary field obtained by either distributions is very omnidirectional, with almost constant SPLs in both

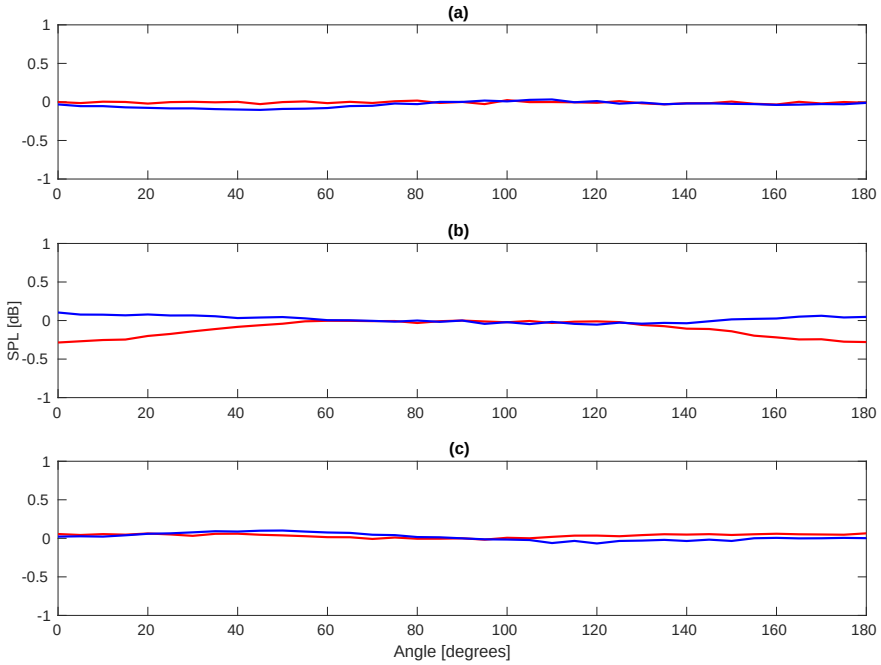

Figure 3: Far-field for the force-equilibrium (blue line) and for the equal-area (red line) OPL. Half orbits around the (a) equator, (b) a meridian and (c) with an inclination of 45°. Sound pressure leves are normalized with respect to the value at 90^o, where the three trajectories cross.

cases. On the other hand, this theoretical model also helped us to determine a proper sphere radius. This was selected to $R = 0.125$ m, since the predicted directivity pattern and sound pressure levels were good enough for our purposes while keeping a reasonable number of transducers.

In summary, the OPL was designed to have 750 PZT transducers (Multicomp 16mm Transmitter (ST160)) distributed on a sphere of radius $R = 0.125$ m following an equal-area partitioning strategy.

3.2 Spherical casing

The spherical casing of the OPL had to fulfill with the following construction requirements. First, its interior had to be accessible so as to wire and sold all transducers. Second, the exact location of the transducers should be somehow marked in the casing to avoid deviations with respect to the theoretical design. Third, the prototype had to be rigid and consistent enough to resist user manipulation without damage. Fourth, the resulting prototype shall be supported with a microphone stand.

We have complied with the above requirements with a design that splits the sphere into 6 pieces (see Figure 4); 4 pieces for the laterals and 2 for the spherical caps, which greatly simplifies the wiring and soldering of the transducers. The two caps were easy to determine because the equal-area strategy ensures that all the transducers are aligned in a parallel. However, this task was more difficult for the lateral pieces. If we look along any meridian we will find that the transducers are not aligned. The lateral pieces were thus divided in a way that avoided transducers to lie between two different pieces. Besides, each piece contains the exact location of the transducers, the transducer base and the two holes for the pins being marked on the piece surface.

All six pieces can be joined to form the spherical casing, as if it were the six pieces of a puzzle. However, with that configuration the resulting structure was not rigid enough. To get more stiffness some additional pieces were designed. This resulted in a central piece located in the center of the sphere, which is connected to all surface pieces through bars (see Figure 4b) and prevents the surface pieces from collapsing within the sphere. On the other hand, the bottom spherical cap contains a hole that is connected to this central piece. A microphone stand can be introduced there, up to the center of the spherical casing, which ensures a high stability. All the casing pieces were 3D-printed in white color. They were small enough so as to be printable in any regular commercial 3D printer.

(a) (b)

Figure 4: Spherical casing (a) before and (b) after setting the transducers on it. In (b) one of the lateral pieces is removed to better observe the interior.

3.3 Circuitry

As detailed in section 3.2, the spherical casing of the OPL was divided into 6 pieces. All pieces were star-form electrically connected from the central connector of the OPL, as shown in Figure 5. All transducers in the OPL pieces were connected in parallel.

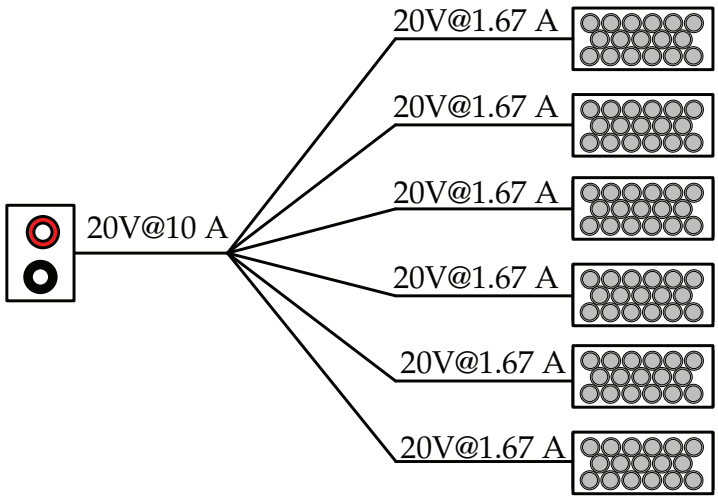

Figure 5. Scheme of the internal wiring of the OPL

Two types of wiring were used in the connection design. On the one hand, a naked wiring for connecting all the transducers in a piece. The wire has a section of $0.2\mathrm{mm}^2$, which allows a maximum current of 15 A, and completely suffices for the 1.67 A current flow needed for each piece (this corresponds to a sixth of the total 10 A current for the OPL). The union of the transducers within each piece was zigzagged to minimize the length of the wiring, thus simplifying the welding process. On the other hand, a second type of wire with section $1\mathrm{mm}^2$ (suitable for currents up to 20 A) was employed to connect the six pieces as described in Figure 5.

The setup scheme of the OPL is shown in Figure 6. A passive protection circuit has been designed to be inserted between the power amplifier (Ecler XPA3000) and the OPL. This circuit protects the entire set of both, overvoltage and overcurrent, avoiding possible damage to the OPL and also to the power amplifier. The protection circuit contains a relay that selects the most suitable path between the OPL and a resistive load (whose impedance is recommended by the manufacturer of the amplifier). The second path (through the resistive load) is activated when the peak envelope is higher than a predetermined threshold, settled to 20 V.

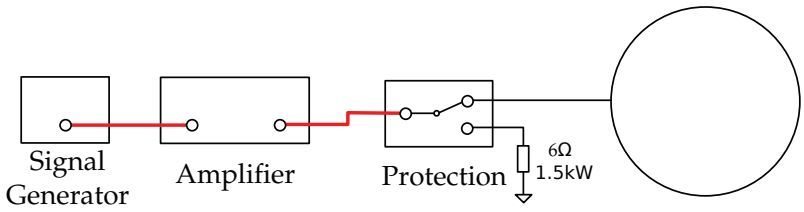

Figure 6. Scheme of the setup of the OPL

4 EXPERIMENTAL TESTING

The directivity pattern of the OPL was measured within the anechoic chamber of La Salle, Universitat Ramon Llull (see Figure 7). Pure tones, of frequency equal to the central frequencies of

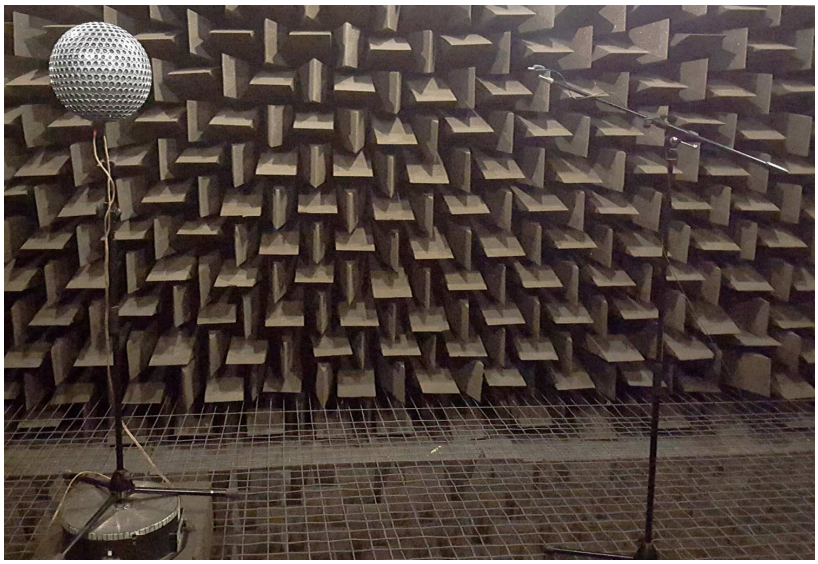

Figure 7. Experimental setup used to measure the directivity pattern of the OPL.

1/1 octave-bands from 250 Hz to 8 kHz, were emitted while the OPL rotated continuously from 0^{o} to 360^{o} by means of a turntable. Each pure tone was modulated with Upper Side Band Amplitude Modulation (USBAM) and emitted trough a Data Translation 9832 card. This signal was amplified using an Ecler XPA3000 with an input voltage of 16 Vpeak. This value was selected to avoid to damage the OPL, as it is clearly below the maximum voltage of 20 Vrms that the ultrasound transducers can tolerate. The generated sound pressure levels were measured with a free field microphone 1/4 inch (G.R.A.S. 40BF) and recorded with the acquisition card through a Nexus conditioning amplifier. The microphone was located at 1 meter distance from the OPL. For comparison purposes, the directivity pattern of a conventional dodecahedral loudspeaker was also measured using the same experimental setup. In this case the pure tones were emitted without modulation.

Figure 8 presents the experimental results obtained for the directivity pattern of the OPL and the conventional dodecahedral loudspeaker, with a resolution of 1^{o}. The results are expressed in the usual polar representation and normalized to the mean sound pressure level for each frequency. In addition, the Directivity Index (DI) is also computed from each directivity pattern as described in the ISO 16283-1 [17]. This is defined as

$$DI_i = L_{360^{\text{o}}} - L_{30,i}, \tag{7}$$

with $L_{360^{\text{o}}}$ being the mean pressure value along the arc from 0^{o} to 360^{o}, and $L_{30,i}$ the mean pressure value along a 30^{o} arc. The i index indicates the different intervals that cover each 30^{o} arc, that is, from 0^{o} to 30^{o}, from 30^{o} to 60^{o}, etc.

As can be observed in Figure 8a, the dodecahedral loudspeaker has a very good omnidirectional behaviour for low frequencies, but for higher ones, above 2 kHz, there are some regions in which the pressure levels can decay up to about -25 dB. As explained in the Introduction, this is produced because the directivity of regular loudspeakers sharpens with increasing frequency, so that acoustic shadow regions appear in the vicinity of the dodecahedron vertices. Looking now at the directivity pattern of the OPL (see Figure 8b), it fluctuates very quickly for all frequencies, compared to the dodecahedral loudspeaker. Moreover, some large pressure drops are also produced.

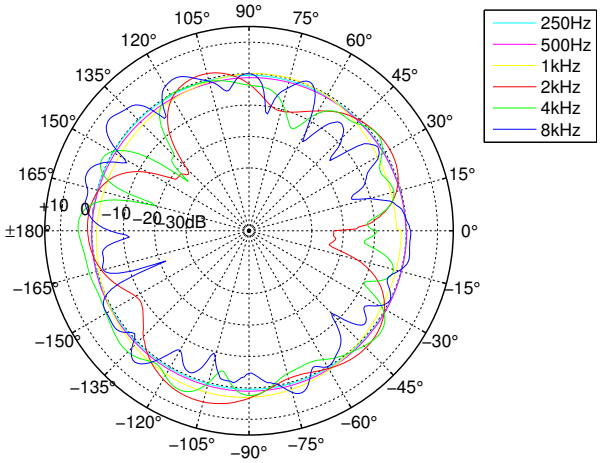

(a) Dodecahedron - Directivity pattern

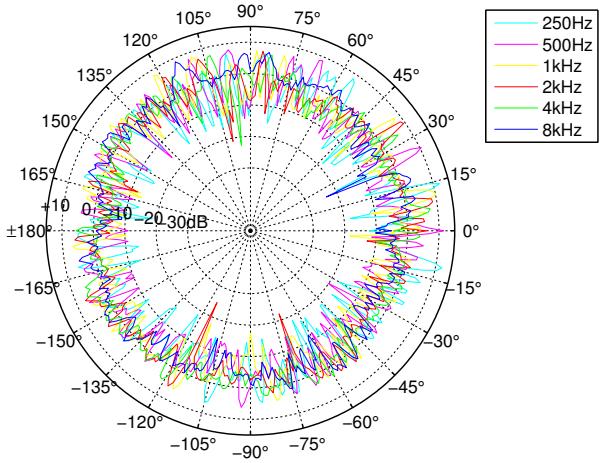

(b) OPL - Directivity pattern

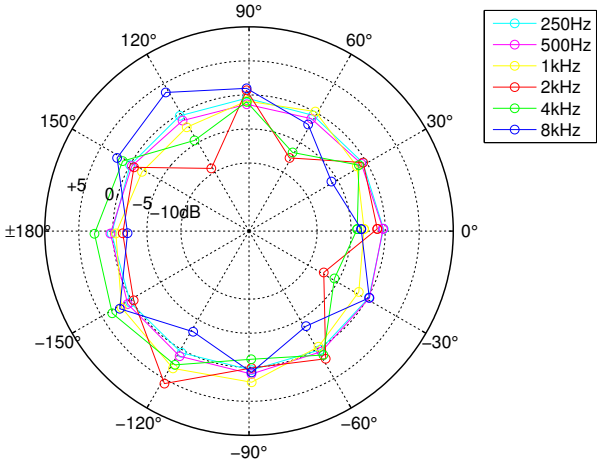

(c) Dodecahedron - Directivity Index

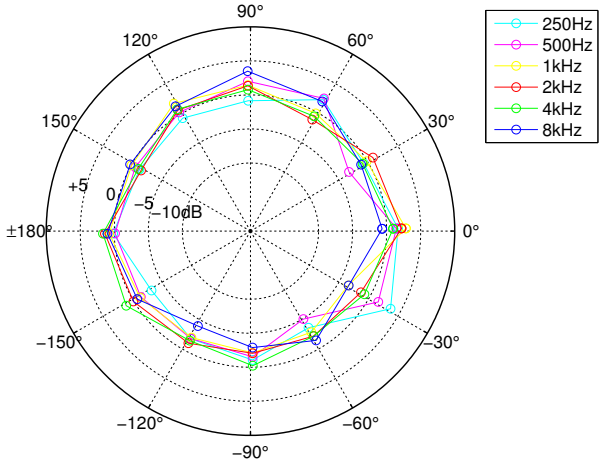

(d) OPL - Directivity Index

Figure 8: Directivity pattern and Directivity Index of a conventional dodecahedral loudspeaker and the OPL.

However, these are focused in narrower areas compared to the dodecahedral loudspeaker, and the fluctuations seem to oscillate along a mean pressure value. The DI can shed light on this point as it relates the mean pressure value along a 30^o arc with the total mean pressure, giving a better idea about the omnidirectionallity of each sound source. Comparing the DI of the OPL against that of the dodecahedral loudspeaker (see Figure 8d and Figure 8c), it can be observed in fact that the OPL is more omnidirectional at higher frequencies than the dodecahedral loudspeaker. On the other hand, note that all the frequency curves are very similar for the OPL, which means that it maintains its omnidirectional behaviour independently of the introduced frequency. In contrast, larger differences can be observed in the DI of the dodecahedral loudspeaker when changing the frequency. However, as it could be expected, this conventional loudspeaker performs better than the OPL for frequencies lower than 2 kHz, since the problem with the dodecahedron vertices does not exist in the low frequency range.

5 CONCLUSIONS

In this work a new omnidirectional parametric loudspeaker prototype was build. 750 piezo-electric transducers were used for this purpose, equally distributed in the parallels of a sphere of radius 0.125 m. 3D-printing technology was employed to construct the 6 pieces that form the spherical casing of the OPL, together with some additional elements that provide robustness. This design greatly simplified the wiring and soldering of all transducers. The OPL prototype was tested in an anechoic chamber. The preliminary results showed that the OPL has an omnidirectional behaviour, although its directivity pattern fluctuates very quickly compared to a conventional dodecahedron loudspeaker. However, when examining the Directivity Index, the OPL presented clear improvements at higher frequencies, although it performed worst for the lower ones. Future works will determine the potential of the OPL to perform standard measurements in building acoustics, such as reverberation time of a room or the airborne sound insulation of a partition. Moreover, more experiments will be performed to better examine the behaviour of this new sound of source.

ACKNOWLEDGMENTS

This work has been supported by the BUILT2SPEC project, which has received funding from the European Union's Horizon 2020 Research and Innovation Program under Grant Agreement no. 637221. The authors acknowledge the support from the Secretaria d'Universitats i Recerca del Departament d'Economia i Coneixement (Generalitat de Catalunya) under grant ref. 2017-SGR-966.

REFERENCES

[1] P. J. Westervelt. Parametric acoustic arrays. *J. Acoust. Soc. Am.*, 35(4):535–537, 1963.

[2] M. F. Hamilton. Sound beams. In *Nonlinear Acoustics: Theory and Applications*, pages 233–261. Academic Press Inc., 1997.

[3] W. Gan, J. Yang, and T. Kamakura. A review of parametric acoustic array in air. *Appl. Acoust.*, 73(12):1211–1219, 2012.

[4] U. Sayin, P. Artís, and O. Guasch. Realization of an omnidirectional source of sound using parametric loudspeakers. *J. Acoust. Soc. Am.*, 134(3):1899–1907, 2013.

[5] M. Yoneyama, Y. Kawamo, J. Fujimoto, and S. Sasabe. The audio spotlight: An application of nonlinear interaction of sound waves to a new type of loudspeaker design. *J. Acoust. Soc. Am.*, 73(5):1532–1536, 1983.

[6] F. J. Pompei. The use of airborne ultrasonics for generating audible sound beams. *J. Audio Eng. Soc.*, 47(9):726, 1999.

[7] H. O. Berktay and D. J. Leahy. Far-field performance of parametric transmitters. *J. Acoust. Soc. Am.*, 55(3):539, 1974.

[8] C. Shi and W. Gan. Product directivity models for parametric loudspeakers. *J. Acoust. Soc. Am.*, 131(3):1938–1945, 2012.

[9] C. Shi and Y. Kajikawa. A convolution model for computing the far-field directivity of a parametric loudspeaker array. *J. Acoust. Soc. Am.*, 137(2):777–784, 2015.

[10] O. Guasch and P. Sánchez-Martín. Far-field directivity of parametric loudspeaker arrays set on curved surfaces. *Submitted*, 2018.

[11] N. Tanaka and M. Tanaka. Active noise control using a steerable parametric array loudspeaker. *J. Acoust. Soc. Am.*, 127(6):3526–3537, 2010.

[12] N. Tanaka and M. Tanaka. Mathematically trivial control of sound using a parametric beam focusing source. *J. Acoust. Soc. Am.*, 129(1):165–172, 2011.

[13] U. Sayin and O. Guasch. Directivity control and efficiency of parametric loudspeakers with horns. *J. Acoust. Soc. Am.*, 134(2):EL153–EL157, 2013.

[14] E. B Saff and A. BJ Kuijlaars. Distributing many points on a sphere. *Math. Intell.*, 19(1):5–11, 1997.

[15] A. Katanforoush and M. Shahshahani. Distributing points on the sphere, I. *Exper. Math.*, 12(2):199–209, 2003.

[16] P. Persson and G. Strang. A simple mesh generator in matlab. *SIAM review*, 46(2):329–345, 2004.

[17] ISO 16283-1. *Acoustics—Field measurement of sound insulation in buildings and of building elements — Part 1: Airborne sound insulation*. International Organisation for Standardization, Geneva, Switzerland, 1998.